# Regulation of Connexin32 by ephrin receptors and T-cell protein-tyrosine phosphatase

Received for publication, May 8, 2018, and in revised form, October 25, 2018 Published, Papers in Press, November 6, 2018, DOI 10.1074/jbc.RA118.003883

**Andrew J. Trease**[‡1], **Hanjun Li**[‡§1], **Gaelle Spagnol**[‡], **Li Zheng**[‡], **Kelly L. Stauch**[‡], **and Paul L. Sorgen**[‡2]

*From the* [‡]*Department of Biochemistry and Molecular Biology and* [§]*Eppley Institute for Research in Cancer and Allied Diseases, University of Nebraska Medical Center, Omaha, Nebraska 68198*

Edited by Wolfgang Peti

**Gap junctions are intercellular conduits that permit the passage of ions, small metabolites, and signaling molecules between cells. Connexin32 (Cx32) is a major gap junction protein in the liver and brain. Phosphorylation is integral to regulating connexin assembly, degradation, and electrical and metabolic coupling, as well as to interactions with molecular partners. Cx32 contains two intracellular tyrosine residues, and tyrosine phosphorylation of Cx32 has been detected after activation of the epidermal growth factor receptor; however, the specific tyrosine residue and the functional implication of this phosphorylation remain unknown. To address the limited available information on Cx32 regulation by tyrosine kinases, here we used the Cx32 C-terminal (CT) domain in an *in vitro* kinase-screening assay, which identified ephrin (Eph) receptor family members as tyrosine kinases that phosphorylate Cx32. We found that EphB1 and EphA1 phosphorylate the Cx32CT domain residue $Tyr^{243}$. Unlike for Cx43, the tyrosine phosphorylation of the Cx32CT increased gap junction intercellular communication. We also demonstrated that T-cell protein-tyrosine phosphatase dephosphorylates $pTyr^{243}$. The data presented above along with additional examples throughout the literature of gap junction regulation by kinases, indicate that one cannot extrapolate the effect of a kinase on one connexin to another.**

Gap junctions are intercellular channels that permit the free passage of ions, small metabolites, and signaling molecules between neighboring cells. They are important for a number of physiological processes, including cell growth, differentiation, and synchronization. A major gap junction protein in the liver and brain, as well as in a number of other tissues, is Connexin32 (Cx32)[3] (1). Cx32-deficient mice have an increased chance of developing spontaneous liver tumors and are more vulnerable to chemical-induced liver tumorigenesis (2, 3); these mice exhibit other pathological phenotypes, such as decreased nerve-dependent bile secretion, enhanced pancreatic amylase secretion, and peripheral nerve demyelination (4–7). Since identifying Cx32 as an X-linked Charcot-Marie-Tooth disease–causing protein, more than 400 different mutations affecting every region of the Cx32 protein have been reported (8). These mutations alter trafficking to the plasma membrane, channel gating, channel selectivity, protein partner interactions, and the phosphorylation status (9).

All stages of the connexin life cycle, which include assembly, degradation, the regulation of electrical and metabolic coupling, and regulation of interactions with molecular partners, involve phosphorylation (10). Cx32 contains 12 serine residues within the cytoplasmic domains that are enzyme-accessible (N-terminal (NT) domain, 2 residues; cytoplasmic loop, one residue; C-terminal (CT) domain, 9 residues) and is *in vitro*–phosphorylated by $Ca^{2+}$/calmodulin-dependent protein kinase II, protein kinase A (PKA), and protein kinase C (PKC) (11–13). For the MAP kinase p38, a correlation was made between the differentiation of rat mammary epithelial cells and Cx32 phosphorylation; unfortunately, direct phosphorylation of Cx32 was not tested (14). Cx32 also contains two intracellular tyrosine residues (NT, $Tyr^{7}$; CT, $Tyr^{243}$). Of note, $Tyr^{211}$ may or may not be accessible to the cytosol based on its juxtaposed location to the membrane; however, accessibility would not be favorable to protein interactions. Tyrosine phosphorylation of Cx32 was induced in purified liver membranes by the epidermal growth factor receptor (EGFR) kinase, and the presence of the Cx32-binding partner calmodulin (CaM) inhibited tyrosine phosphorylation (11, 15). Unfortunately, the site(s) of Cx32 phosphorylation by EGFR and its relevance to Cx32 function was not established (11). Finally, Y7 phosphorylation was observed by MS from Cx32-transfected HeLa cells; however, the kinase involved was not identified (16). Based upon the limited available information about Cx32 regulation by tyrosine kinases, we used an *in vitro* kinase-screening assay, which identified the ephrin type-B receptor 1 (EphB1) and ephrin type-A receptor 1 (EphA1) as novel tyrosine kinases that phosphorylate Cx32.

Eph receptors and ligands are both membrane-bound; thus, binding and activation requires cell-to-cell contact. Downstream

This work was supported by NIGMS, National Institutes of Health, Grants GM072631 and GM103427 and by Grant HL131712 from NHLBI, National Institutes of Health. The authors declare that they have no conflicts of interest with the contents of this article. The content is solely the responsibility of the authors and does not necessarily represent the official views of the National Institutes of Health.

This article contains Figs. S1 and S2.

[1] Both authors contributed equally to this work.

[2] To whom correspondence should be addressed: Dept. of Biochemistry and Molecular Biology, University of Nebraska Medical Center, Omaha, NE 68198. Tel.: 402-559-7557; Fax: 402-559-6650; E-mail: psorgen@unmc.edu.

[3] The abbreviations used are: Cx32, Connexin32; NT, N-terminal; CT, C-terminal; PKA, protein kinase A; PKC, protein kinase C; MAP, mitogen-activated protein; EGFR, epidermal growth factor receptor; CaM, calmodulin; GJIC, gap junction intercellular communication; TC-PTP, T-cell protein-tyrosine phosphatase; DTSSP, 3,3′-dithiobis(sulfosuccinimidylpropionate); IP, immunoprecipitation; HSQC, heteronuclear single quantum correlation; SAP97, synapse-associated protein 97; Eph, ephrin; RT, room temperature; TX-100, Triton X-100; ANOVA, analysis of variance; DAPI, 4′,6-diamidino-2-phenylindole.

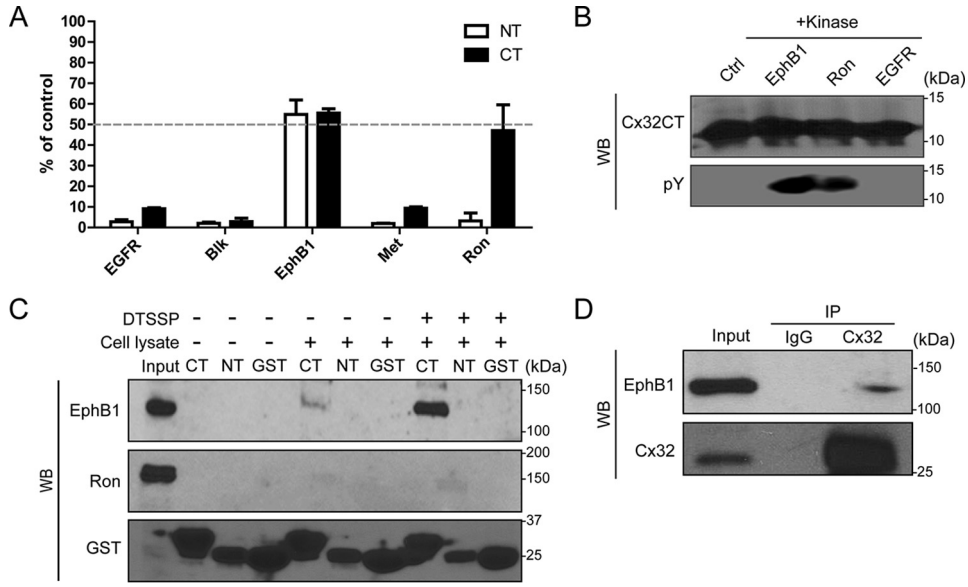


**Figure 1. EphB1 phosphorylates the Cx32CT domain *in vitro*.** *A*, the Cx32NT and CT domains were used as a substrate for the human EGFR, Blk, EphB1, Met, and Ron kinases (performed by Eurofin Scientific). The amount of Cx32NT and CT phosphorylation was compared with a positive control peptide for each kinase (percentage of control signal). The *dashed line* highlights 50% of the control signal. *B*, an *in vitro* kinase assay for the Cx32CT was performed in our laboratory to repeat the kinase screen performed by Eurofin Scientific (EphB1, Ron, and EGFR). A general anti-phosphotyrosine antibody was used to detect the phosphorylation level by Western blotting (*WB*). The control group used buffer to substitute the kinases in the reactions. *C*, purified GST alone, GST-Cx32CT (*CT*), or GST-Cx32NT (*NT*) bound on GSH-agarose beads was incubated without (−) or with (+) HeLa cell lysate, and the pulled down proteins were analyzed by Western blotting using anti-EphB1 or anti-Ron antibodies. The chemical cross-linker DTSSP was used to capture the weak and/or transient interactions. *D*, co-IP was performed in HeLa cells stably expressing Cx32. Lysates were immunoprecipitated with anti-Cx32 or IgG and then blotted for Cx32 and EphB1. *Error bars*, S.D.

signaling is important for proper cell sorting during development, cell adhesion, migration, repair after nervous system injury, and maintenance of gap junctions (17–20). The EphB4 receptor co-immunoprecipitated with Cx43, and its activation in primary cultures of rodent cardiomyocytes inhibited gap junction intercellular communication (GJIC) (21). Another study showed that GJIC is inhibited at ectopic ephrin boundaries and that ephrin-B1 physically interacts with Cx43 and influences its distribution (19). Altogether, these studies suggest a mechanism by which Eph receptors and ligands mediate control of cell-to-cell communication through phosphorylation of the gap junction proteins. Nevertheless, whether the Eph receptors directly phosphorylate connexins and whether this is a general mechanism to regulate other connexin isoforms remain to be determined.

Here, we identified that the Eph receptor isoforms EphB1 and EphA1 phosphorylate Cx32CT residue $Tyr^{243}$, an event that increases GJIC. We also demonstrate that the T-cell protein-tyrosine phosphatase (TC-PTP) dephosphorylates Cx32CT residue $pTyr^{243}$. This study provides evidence that characterization of the same kinase for different connexin isoforms is important, as one cannot extrapolate the effect of a kinase on one connexin to another.

## Results

### *EphB1 directly interacts and phosphorylates the Cx32CT domain*

GPS 2.0, NetPhos 2.0 server, and KinasePhos 2.0 were used to predict tyrosine kinases that could phosphorylate the Cx32 NT and CT domains. Five tyrosine kinases were selected for an *in vitro* tyrosine phosphorylation screening assay performed by Eurofins Scientific (KinaseProfiler) using the Cx32NT ($Met^1$–$Gly^{21}$; $Tyr^7$) or the Cx32CT ($Cys^{217}$–$Cys^{283}$; $pTyr^{243}$) as substrates (Fig. 1*A*). Of the kinases tested, EphB1 and Ron resulted in phosphorylation of the Cx32CT greater than 50 and 40% of control peptide signal, respectively. EphB1 was the only kinase able to phosphorylate the Cx32NT and did so to a level similar to that of the Cx32CT. To validate the screen results, the kinase assay was repeated using EphB1, Ron, and EGFR in our laboratory. Consistent with data from Eurofins Scientific, EphB1 and Ron phosphorylated Cx32CT residue $pTyr^{243}$ but not EGFR (Fig. 1*B*). Of note, work from Diez *et al.* (11) demonstrated that EGFR can phosphorylate immunoprecipitated Cx32 *in vitro* as detected by autoradiography.

To confirm the Cx32 interaction with the EphB1 and Ron kinases, a pulldown assay was performed using purified GST, GST-Cx32NT, or GST-Cx32CT and lysate from HeLa cells expressing EphB1 and Ron (but not Cx32) (Fig. 1*C*). EphB1 was pulled down by GST-Cx32CT, but not GST or GST-Cx32NT. The EphB1 interaction with the Cx32CT was stabilized by the chemical cross-linker 3,3′-dithiobis(sulfosuccinimidylpropionate) (DTSSP), which can capture weak and/or transient interactions (22)). Co-immunoprecipitation (co-IP) showed that EphB1 is in the same complex with full-length Cx32 (Fig. 1*D*). Conversely, whereas Ron could phosphorylate the Cx32CT *in vitro*, the interaction was weak in the pulldown assay (even in the presence of DTSSP) and not detected by co-IP (data not shown). Thus, Ron was excluded from further experimentation, highlighting a caveat in this type of *in vitro* screen where the phosphorylation *in vitro* does not always correlate with a detectable interaction in cells.

### *TC-PTP interacts with and dephosphorylates Cx32CT residue $pTyr^{243}$*

Previously, we identified that TC-PTP directly dephosphorylated Cx43 on the CT domain, leading to increased GJIC (23).

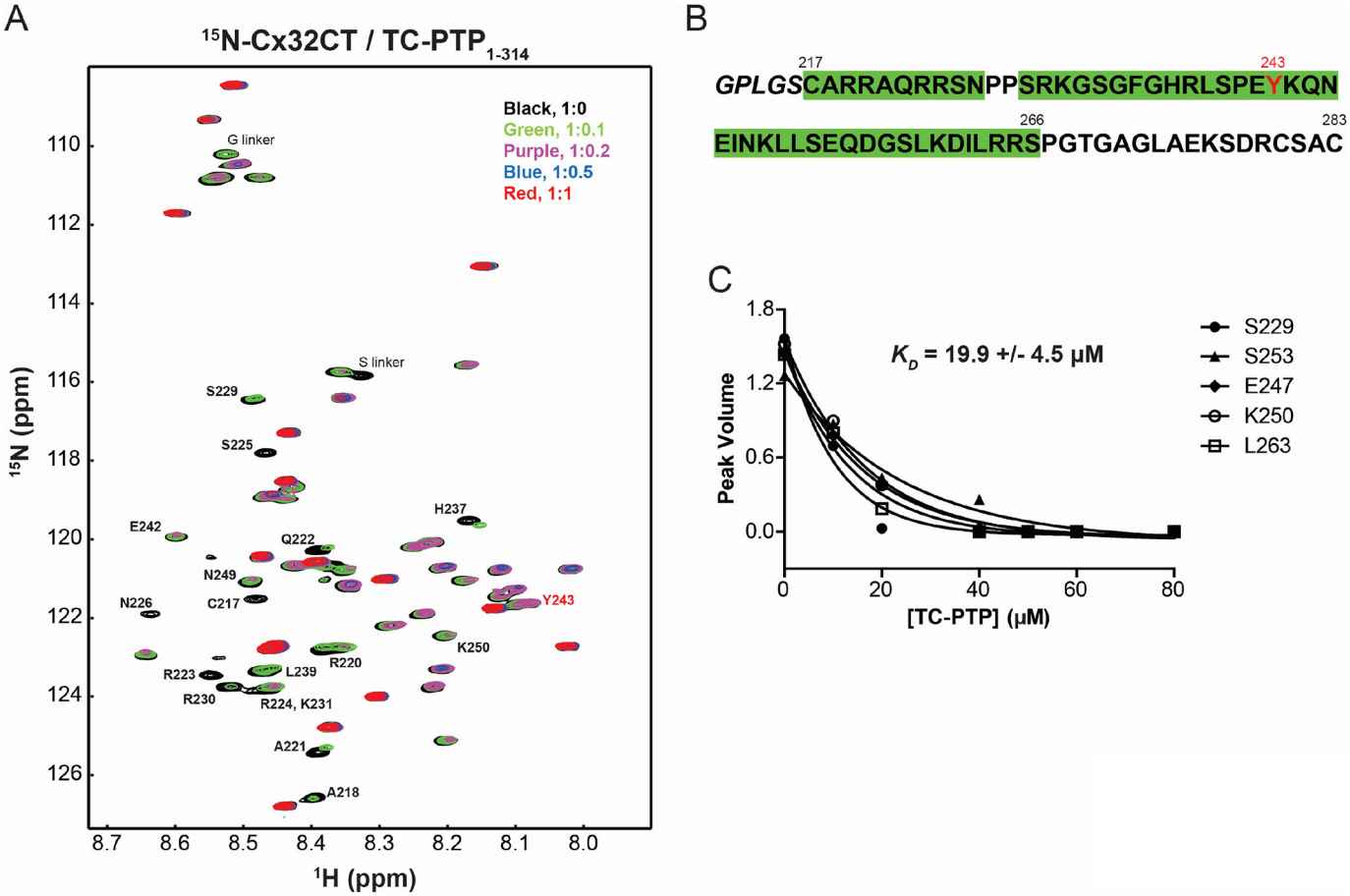


**Figure 2. Cx32CT residues affected by the direct interaction with TC-PTP.** *A*, overlaid $^{15}$N HSQC spectra of the [$^{15}$N]Cx32CT alone (residues 217–283; 30 $\mu$M) and in the presence of different concentrations of unlabeled TC-PTP(1–314). The *cross-peak color* changes according to the concentration ratio. The strongly affected peaks are *labeled*. *B*, amino acid sequence of Cx32CT. Residues affected by the addition of TC-PTP(1–314) are *highlighted* in *green*. Shown in *red* is Cx32 residue Tyr$^{243}$. *C*, $K_D$ for the TC-PTP(1–314) interaction with Cx32CT was estimated by fitting the decrease in signal intensity as a function of TC-PTP(1–314) concentration. Represented is a subset of the residues used to calculate the $K_D$.

Whether TC-PTP can dephosphorylate other connexin isoforms (*e.g.* Cx32 pTyr$^{243}$) is unknown. To determine whether a direct interaction exists between TC-PTP and the Cx32CT domain, NMR titration experiments were performed with the purified TC-PTP catalytic domain (TC-PTP(1–314)) and Cx32CT. Different concentrations of unlabeled TC-PTP(1–314) were titrated into $^{15}$N-labeled Cx32CT (residues Cys$^{217}$–Cys$^{283}$) and $^{15}$N HSQC spectra were acquired (Fig. 2*A*). By the 1:1 molar ratio, Cx32CT residues Cys$^{217}$–Ser$^{266}$ (including Tyr$^{243}$) had broadened beyond detection (*highlighted* on the Cx32CT sequence in Fig. 2*B*; *red*). The decrease in signal intensity from increasing TC-PTP(1–314) concentrations was fit according to the nonlinear least square method, and the binding affinity ($K_D$) for the interaction was determined to be 19.9 ± 4.5 $\mu$M (Fig. 2*C*). A GST pulldown experiment was performed to validate the NMR results. Purified GST alone, GST-Cx32CT, or GST-Cx32NT bound to GSH-Sepharose was incubated with purified TC-PTP(1–314). Immunoblotting using an anti-TC-PTP NT antibody identified that GST-Cx32CT, but not NT, directly interacted with the TC-PTP catalytic domain (Fig. 3, *A* and *B*). GST-Cx32CT also pulled down full-length TC-PTP from HeLa cell lysate (Fig. 3*C*).

To determine whether TC-PTP dephosphorylates the Cx32 on residue Tyr$^{243}$, an *in vitro* phosphatase assay was conducted using a peptide (His$^{237}$–Asn$^{249}$) containing pTyr$^{243}$ incubated with TC-PTP(1–314). Following the protocol for the Malachite green assay (Millipore), an increase in the amount of $P_i$ production was observed, indicating that TC-PTP dephosphorylated the Cx32 peptide on pTyr$^{243}$ (Fig. 3*D*). Notably, TC-PTP has a comparable affinity for both the Cx32 peptide and positive control, as shown by the kinetic data in Table 1 ($k_{cat}/K_m \cdot 10^{-6}$; 2.24 ± 0.18 *versus* 2.42 ± 0.47).

### *EphB1 phosphorylates and TC-PTP dephosphorylates Cx32 in HeLa cells*

We have shown that EphB1 phosphorylates and TC-PTP dephosphorylates Cx32 *in vitro*. To determine whether EphB1 and TC-PTP affect the level of Cx32 pTyr$^{243}$ in cells, HeLa cells stably expressing Cx32 WT were transfected with EphB1 and/or the TC-PTP catalytic domain (residues 1–314), and the tyrosine phosphorylation level was detected on immunoprecipitated Cx32 (Fig. 4*A*). No tyrosine phosphorylation of Cx32 was detected in the control lane (no transfection of EphB1 or TC-PTP(1–314)). Expression of EphB1 increased Cx32 tyrosine phosphorylation and double transfection with TC-PTP(1–314) decreased Cx32 tyrosine phosphorylation when compared with only EphB1.

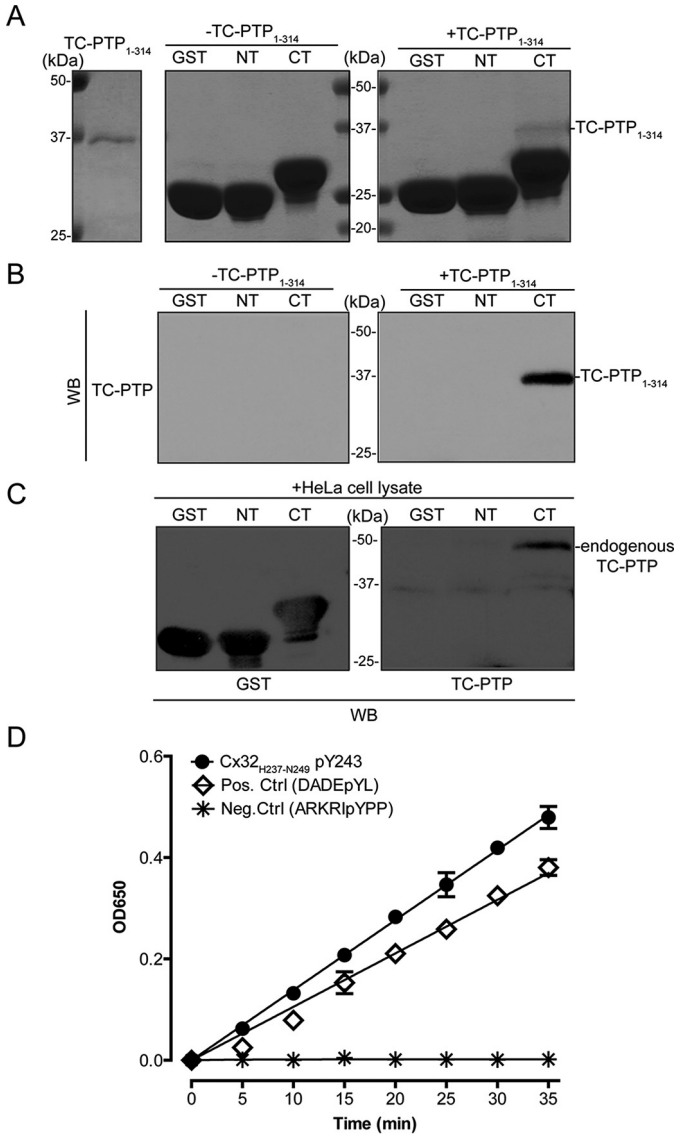


**Figure 3. TC-PTP interacts with the Cx32CT domain and dephosphorylates pTyr$^{243}$.** *A*, purified GST, GST-Cx32NT, or GST-Cx32CT on GSH-Sepharose beads was incubated without (−) or with (+) purified TC-PTP catalytic domain (residues 1–314). After washes, samples were run on an SDS-polyacrylamide gel and stained with Coomassie Blue. *B*, GST pulldown samples were blotted (*WB*) with the anti-TC-PTP NT antibody. The TC-PTP catalytic domain is 36 kDa. *C*, purified GST, GST-Cx32NT, or GST-Cx32CT bound on GSH beads were incubated with HeLa cell lysate containing endogenous TC-PTP. Pulled down proteins were analyzed by Western blotting using anti-TC-PTP NT or anti-GST antibodies. *D*, plot of the Malachite green assay shows the time course of Cx32 phosphopeptides containing pTyr$^{243}$ dephosphorylated by the TC-PTP catalytic domain (1.2 nmol). Data were recorded based on readings at $A_{650}$. Each experiment was repeated three times. *Error bars*, S.D.

**Table 1**

**Kinetic constants for dephosphorylation of Cx32 pTyr$^{243}$ by TC-PTP(1–314)**

| | $K_m$ | $k_{cat}$ | $k_{cat}/K_m \cdot 10^{-6}$ |
|---|---|---|---|
| | $m_M$ | $s^{-1}$ | $M^{-1}s^{-1}$ |
| Positive control[a,b] | 0.022 ± 0.001 | 52.8 ± 10.6 | 2.42 ± 0.47 |
| pTyr$^{243}$[a] | 0.028 ± 0.007 | 63.3 ± 13.8 | 2.24 ± 0.18 |

[a] All data were collected at pH 7.5, 25 °C.
[b] Notably, the kinetic constants determined for the positive control (DADEpYL) by TC-PTP(1–314) are constants with a previous report of the same peptide with PTP1B catalytic domain, whose sequence is very similar to TC-PTP(1–314) (52).

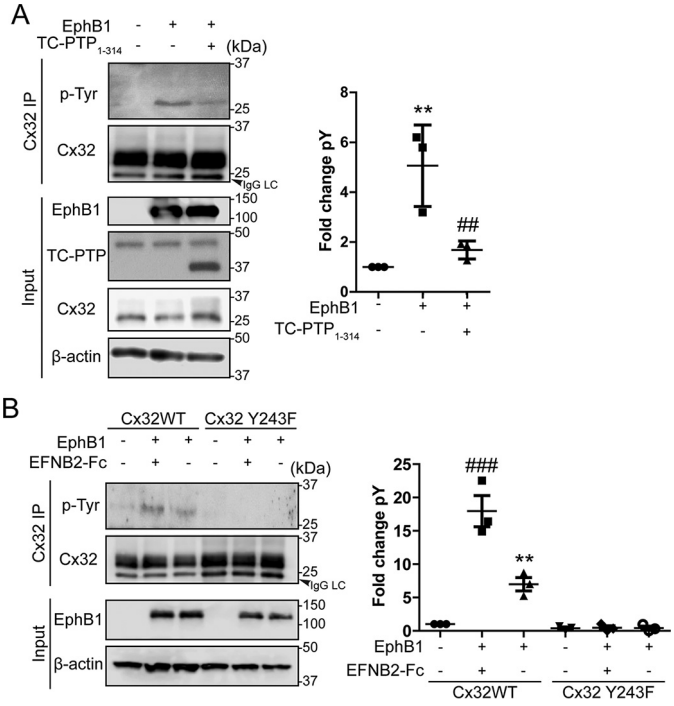


**Figure 4. EphB1 increases and TC-PTP decreases the tyrosine phosphorylation level on Cx32.** *A*, HeLa cells stably expressing Cx32 were transfected with EphB1 and/or the TC-PTP catalytic domain (residues 1–314). Cx32 was immunoprecipitated, and tyrosine phosphorylation was detected with a general phosphotyrosine antibody. The level of tyrosine phosphorylation was quantified by densitometry from three independent experiments. **, $p <$ 0.01 (compared with control); ##, $p < 0.01$ (compared with ephrin-B1) (one-way ANOVA). *B*, HeLa cells stably expressing Cx32 WT or the Y243F mutant were transfected with EphB1. Ephrin-B2-Fc was used to activate the EphB1 receptor. Cx32 was immunoprecipitated, and the level of tyrosine phosphorylation was detected by Western blotting. **, $p < 0.01$ (compared with control); ###, $p <$ 0.001 (compared with ephrin-B1) (one-way ANOVA). *Black arrows*, IgG light chain. *Error bars*, S.D.

Although an interaction between Cx32NT and EphB1 was not observed by GST pulldown (Fig. 2), phosphorylation of Cx32NT residue Tyr$^7$ by EphB1 was observed *in vitro*; thus, we tested whether this residue could be phosphorylated in HeLa cells (16). Cx32 was immunoprecipitated from HeLa cells stably expressing Cx32 WT or Y243F, and the level of tyrosine phosphorylation was measured (Fig. 4*B*). Expression of EphB1 increased Cx32 WT phosphorylation, which was further increased when EphB1 was activated by the addition of the ligand, EphB2-Fc. However, this effect was not observed in cells expressing the Cx32 Y243F mutant, suggesting that EphB1 only phosphorylates Cx32CT on residue Tyr$^{243}$ (not Tyr$^7$ or Tyr$^{211}$).

### *Cx32 Y243E increases GJIC*

Well-appreciated in the gap junction field is the use of Asp or Glu substitutions as a mimetic for phosphorylation (*e.g.* see Refs. 24 and 25). These substitutions allow for the precise control of the site(s) modified and the production of enough phosphorylated protein to observe the intended biological response. Here, HeLa cells either transiently or stably expressing Cx32 WT or Y243E were used to determine the functional significance of Tyr$^{243}$ phosphorylation on GJIC. Western blotting determined that the expression level of Cx32 WT was twice that of Y243E (Fig. 5*A*). Next, immunofluorescence was used to identify the cellular location of Cx32 (Fig. 5*B*). The Cx32 Y243E

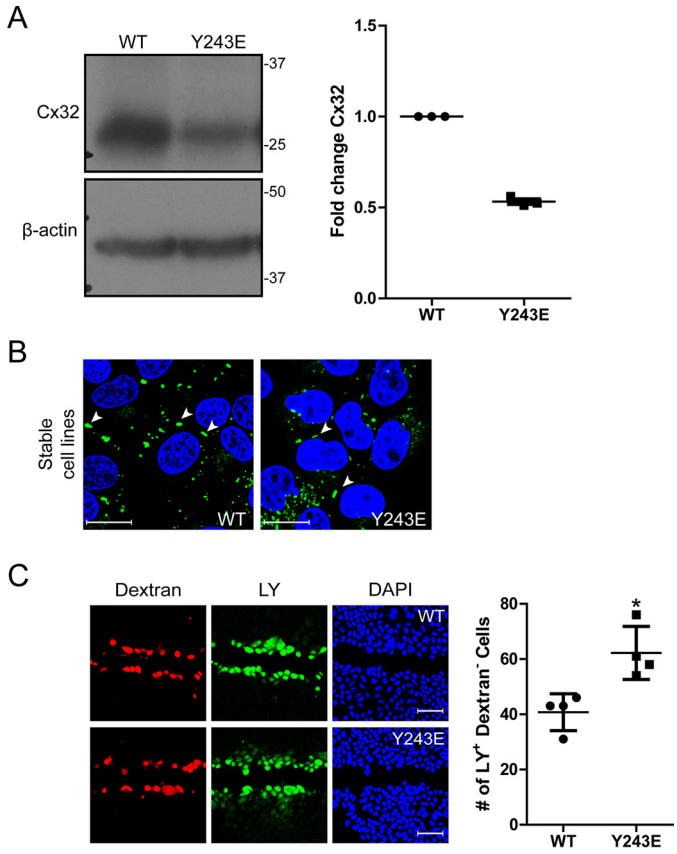


**Figure 5. Cx32 Y243E increases GJIC.** *A*, Western blotting of Cx32 expression in stable Cx32 WT and Y243E HeLa cells. *B*, immunostaining of Cx32 WT and Y243E in stably expressed HeLa cells. *Green*, Cx32; *blue*, DAPI. *White arrow*, gap junction plaques. *Scale bar*, 20 $\mu$m. *C*, GJIC of Cx32 WT and Y243E were investigated using the scrape-loading dye transfer assay. Cells grown on glass coverslips were scrape-loaded with Lucifer yellow (*LY*, *green*) and Texas Red–conjugated dextran (*red*). Nuclei were stained by DAPI to show the confluence of cells. *Scale bar*, 100 $\mu$m. *, $p < 0.01$ (*t* test). *Error bars*, S.D.

mutant formed gap junctions similar to WT at the plasma membrane (*white arrows*). To determine the effect on cell-to-cell communication, the junctional transfer of the fluorescent tracer Lucifer yellow ($M_r$ 443; −2 charge) was measured in a scrape-loading assay (Fig. 5*C*). Interestingly, whereas Cx32 WT protein expression was double that of Y243E and formed plaques of similar size to Y243E, the level of intercellular communication is significantly increased for Y243E. The data suggest that the phosphorylation state of $Tyr^{243}$ can modulate GJIC.

### *EphA1 also phosphorylates Cx32 on the CT domain*

Having established that EphB1 phosphorylates Cx32, we next sought to determine whether different Eph receptor family members could also phosphorylate Cx32. To address this, we again used purified recombinant Cx32CT ($Cys^{217}$–$Cys^{283}$; $Tyr^{243}$) as a substrate for an *in vitro* kinase screen to other Eph receptor family members (Eurofins Scientific; KinaseProfiler). EphB1 and Yes were used as positive and negative controls, respectively. Interestingly, the only other Eph receptor to phosphorylate the Cx32CT was EphA1, which yielded ~67% of control peptide signal (Fig. 6*A*). HeLa cells stably expressing Cx32 were then transiently transfected with cDNA coding human EphA1, and after expression, the receptor was activated with soluble ephrin-A1-Fc. Similar to EphB1, activation of EphA1 caused a significant increase in Cx32 tyrosine phosphorylation (Fig. 6*B*). Next, we determined whether phosphorylation of Cx32 by EphA1 would occur in Caco2 cells (human colon cancer), which endogenously expresses both proteins (Fig. 6*C*). Similar to when overexpressed in HeLa cells, a significant increase in Cx32 tyrosine phosphorylation was observed when the Caco2 cells were stimulated with the soluble ephrin-A1 ligand (Fig. 6*D*). The Cx32 Y243E dye transfer data from Fig. 5 would suggest that phosphorylation of Cx32 by EphA1, like EphB1, would lead to increased GJIC. Indeed, when we tested this using Caco2 cells stimulated with the soluble ephrin-A1 ligand, a significant increase in dye transfer was observed when compared with nonstimulated cells (29 *versus* 12 cells receiving dye; Fig. 6*E*). This increase was similar to the Cx32 Y243E cells.

### *Phosphorylation at $Tyr^{243}$ has little to no effect on the Cx32CT interaction with CaM or synapse-associated protein 97 (SAP97)*

A clear relationship exists between phosphorylation of connexin CT residues and the binding of molecular partners, with examples of both increasing and decreasing binding affinities (*e.g.* see Refs. 26 and 27). CaM and SAP97 were previously shown by our laboratory to interact with the Cx32CT in a region covering $Tyr^{243}$ (CaM: $Cys^{217}$–$Ser^{266}$; SAP97: $Cys^{217}$–$Gln^{245}$) (15). Therefore, we tested using NMR $^{15}N$ HSQC titrations whether phosphorylation of $Tyr^{243}$ would affect these interactions. The data indicate that phosphorylation of $Tyr^{243}$ alone does not have a significant impact on the Cx32CT interaction with CaM or SAP97 (Figs. S1 and S2).

The possibility exists that other kinases activated downstream of the Eph receptors would phosphorylate Cx32CT to affect binding of these proteins (*e.g.* all *in vitro*: $Ser^{229}$ (PKC), $Ser^{233}$ (PKA and PKC), and $Ser^{240}$ (PKC)) (12, 16). Another possibility is that the main regulatory role of $Tyr^{243}$ phosphorylation is to affect channel properties. It is tempting to speculate that a mechanism by which CaM mediates the closure of Cx32 gap junction channels is by masking the effect of the phosphate on $Tyr^{243}$ to increase GJIC (28, 29) or preventing phosphorylation in the first place, as was observed in a study showing that tyrosine phosphorylation of Cx32 is inhibited in the presence of CaM (30).

## Discussion

A few studies have investigated the regulation of GJIC by Eph receptors and ephrins; although none have looked at the Cx32 isoform, interestingly, their observations of blocking communication through gap junctions were all the same. For example, the EphB4 receptor co-immunoprecipitated with Cx43, and its activation in primary cultures of rodent cardiomyocytes inhibited GJIC (21). Another study found that ephrin-B1 co-immunoprecipitated with Cx43, and the interaction between EphB2– and ephrin-B1–expressing NIH3T3 cells inhibited GJIC and redistributed Cx43 from the plasma membrane to the cytoplasm (19). Consistent with these observations is that expression of Eph receptors and ephrins in zebrafish cap cells blocked GJIC at the boundary between both cell populations (20). Finally, although GJIC was not evaluated, the presence of Cx36

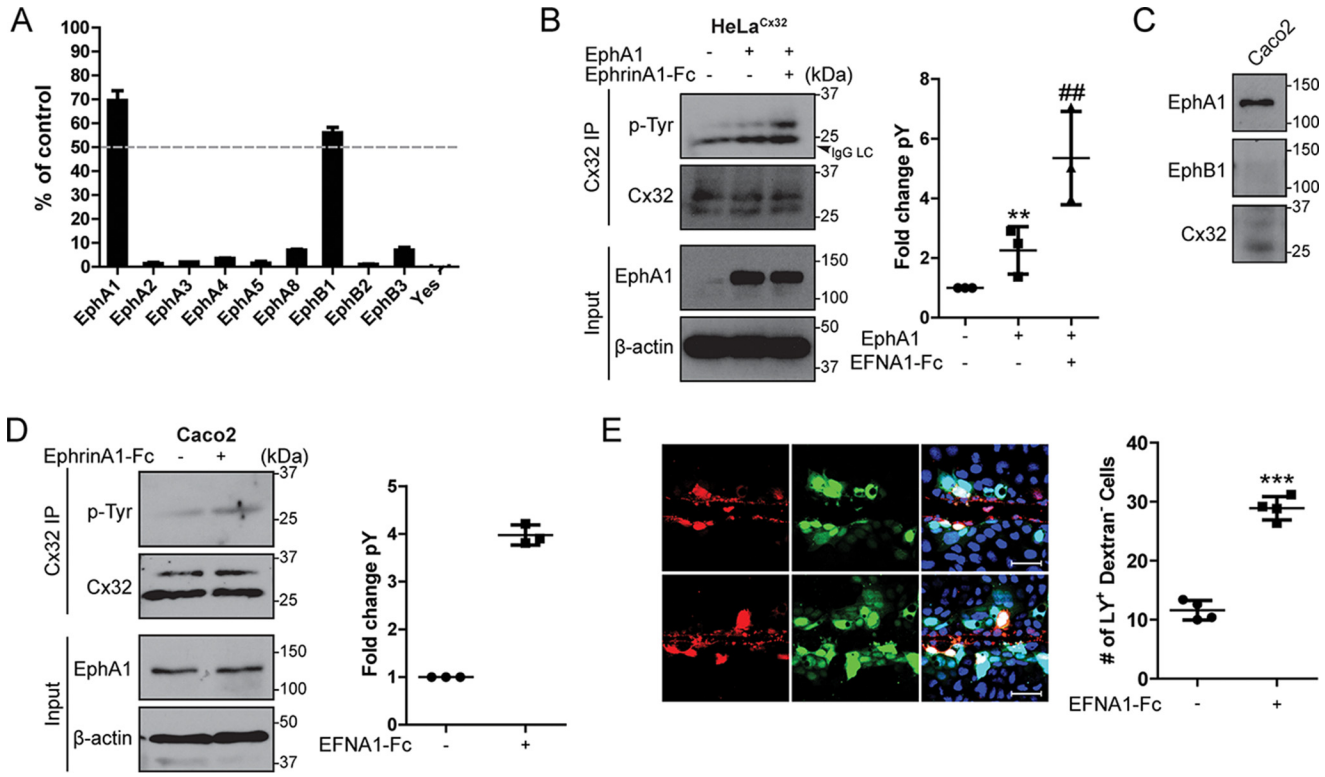


**Figure 6. EphA1 phosphorylation of Cx32 increases gap junction intercellular communication *in vitro* and *in cyto*.** *A*, Cx32CT was used as a substrate for a number of different Eph receptor isoforms. EphB1 and Yes were used as positive and negative control, respectively. The amount of Cx32CT phosphorylation was compared with a positive control peptide for each kinase (percentage of control signal). The *dashed line* highlights 50% of the control signal. *B*, HeLa cells stably expressing Cx32 were transfected with EphA1. Ephrin-A1-Fc was used to activate EphA1 receptor. Cx32 was immunoprecipitated, and the tyrosine phosphorylation level was detected by Western blotting. **, $p < 0.01$ (one-way ANOVA); ##, $p < 0.001$ compared with EphA1. *Black arrows*, IgG light chain. *C*, Western blot analysis of endogenous expression levels of EphA1, EphB1, and Cx32 in Caco2 cells. *D*, Cx32 was immunoprecipitated from Caco2 cells stimulated with ephrin-A1-Fc and probed for tyrosine phosphorylation by Western blotting. *E*, Caco2 cells cultured on glass coverslips were stimulated with ephrin-A1-Fc and scrape-loaded with Lucifer yellow (*LY*, *green*) and Texas Red–conjugated dextran (*red*). Nuclei were stained by DAPI to show the confluence of cells. *Scale bar*, 100 $\mu$m. ***, $p < 0.0001$ (*t* test). *Error bars*, S.D.

was necessary for the effects of EphA on insulin secretion by pancreatic cells (31).

In this study, we identified that EphB1 and EphA1 phosphorylate Cx32CT residue $Tyr^{243}$. Phosphomimetic Cx32 (Y243E) enhanced cell–cell communication in HeLa cells without noticeably affecting the number and size of the gap junction plaque. This observation was substantiated in Caco2 cells, which endogenously express EphA1 (activated by ephrin-A1-Fc) and Cx32. Of note, Cx32 residue $Ser^{233}$ is also associated with increased GJIC when phosphorylated (12). This finding is in contrast to tyrosine phosphorylation of the Cx43CT, as phosphorylation of $Tyr^{247}$, $Tyr^{265}$, and $Tyr^{313}$ is associated with decreased GJIC (10, 32–36). Taken together, this information suggests that phosphorylation (even by the same kinase) regulates different connexin isoforms via different mechanisms. Growing evidence to support this is apparent in the case of regulation by serine kinases, as little correlation exists between Cx43 and Cx45. For example, activation of PKA decreases Cx45 and increases Cx43 junctional conductance (37, 38), and activation of cGMP-dependent protein kinase has no effect on Cx45 but decreases Cx43 junctional conductance (37, 38). Additionally, the response of Cx37 channels to PKC activation or inhibition is opposite to that observed for Cx43 gap junction channels (39).

An important question arises: Where in human anatomy would phosphorylation of Cx32 by Eph receptors occur? Based upon data provided by the Human Protein Atlas, Cx32 is expressed in the appendix, liver, gallbladder, gastrointestinal tract, kidney, and male/female tissues (40) (www.proteinatlas.org/)[4] (51). All of these tissues also express the EphA1 receptor at a similar level. Conversely, the overall expression of EphB1 is relatively low throughout the body; however, like Cx32, EphB1 is highly expressed in the male testis. Activation of EphA1 and EphB1 receptors by their respective ephrins (41) is typically mediated by contact-dependent communication between cells. This is similar to the cell-to-cell contact required for the formation of gap junction channels. Thus, we would hypothesize that under such conditions, phosphorylation of Cx32 would increase GJIC. Additionally, we would expect in any pathological condition where either expression of these proteins is up-regulated or cells that do not normally interact with each other do, Cx32/Eph receptor signaling could occur (18, 42, 43). Although future studies are necessary to address the exact context of Cx32/Eph receptor signaling in human physiology, this study does demonstrate that phosphorylation of the Cx32 residue $Tyr^{243}$, regardless of the kinase, would increase GJIC.

The use of MS, phospho-specific antibodies, mutant versions of connexins eliminating/mimicking phosphorylation, and identification of CT phosphorylation sites has led to the detec-

[4] Please note that the JBC is not responsible for the long-term archiving and maintenance of this site or any other third party hosted site.

tion of phosphorylation-dependent changes in connexin structure, localization, and interacting partners as well as gap junction channel assembly, disassembly, and gating properties (for a review, see Refs. 10 and 44). Through identifying the various cellular conditions and signaling pathways involved in connexin phosphorylation, an understanding of the sequential activation of multiple kinases and changes in the pattern of connexin phosphorylation over time has emerged (*e.g.* see Ref. 10). The significance of defining a connexin phosphorylation pattern under different homeostatic and pathological conditions has the potential to translate this into a therapeutic intervention. Clearly, our understanding of connexin regulation will not be complete until all kinases involved and sites phosphorylated have been identified. The importance of this study is that it directly links phosphorylation of a specific Cx32 tyrosine residue to intercellular communication and provides support for the idea that characterization of the same kinase for different connexin isoforms is important, as the functional significance cannot be inferred from another isoform.

## Experimental procedures

### Cell culture and treatments

Cx32 WT, Y243F, and Y243E were stably expressed in HeLa cells (ATCC). HeLa and Caco2 cells were grown in Dulbecco's modified Eagle's medium (Hyclone, Thermo Fisher Scientific Inc.) supplemented with 10% fetal bovine serum (Hyclone, Thermo Fisher Scientific Inc.) and antibiotics. FHC cells were cultured in Dulbecco's modified Eagle's medium/F-12 supplemented with 25 mM HEPES, 10 ng/ml cholera toxin, 0.005 mg/ml insulin and transferrin, 100 ng/ml hydrocortisone, 20 ng/ml human recombinant EGF, 10% fetal bovine serum, and antibiotics. All cells were cultured in an atmosphere of humidified 5% $CO_2$ at 37 °C. Where appropriate, cells were transiently transfected with either EphA1, EphB1, or a combination of either in conjunction with TC-PTP(1–314) using Lipofectamine 2000 (Invitrogen) according to the manufacturer's protocol. For single and combination transfections, the amount of plasmid for the Eph receptor and TC-PTP(1–314) was equivalent. Cells were treated for 1 h at 37 °C with 1 $\mu$g/ml either EphA1-Fc or EphB2-Fc (SinoBiological) ~24 h after transfection.

### Antibodies and immunostaining

The following antibodies were used in this study: Cx32 mAb (Sigma-Aldrich); Cx32 polyclonal antibody (Life Technologies); EphB1 and EphA1 antibodies (Cell Signaling); TC-PTP antibodies against the N terminus and C terminus (Sigma-Aldrich); nonspecific phosphotyrosine antibody (Cell Signaling).

Cells were immunostained as described previously (45). Briefly, cells grown on coverslips to ~60% confluence were fixed with 2% paraformaldehyde for 15 min. Cells were blocked for 30 min at room temperature (RT) by MPS buffer (1× PBS, 1% goat serum) containing 0.2% TX-100 for permeabilization. Then cells were immunostained with appropriate primary antibodies at RT for 1 h, followed by several PBS plus 0.5% Tween washes. Secondary antibodies (Alexa 594–conjugated goat anti-rabbit antibody and/or Alexa 488–conjugated goat anti-mouse antibody) were applied for 1 h at RT. Images of immunostained cells were acquired with a Zeiss 510 Meta confocal laser scanning microscope using a ×63, 1.4 numerical aperture objective with appropriate filters.

### Co-IP and Western blotting

Cx32-expressing HeLa cells were lysed in complete lysis buffer (50 mM Tris-HCl (pH 7.4), 150 mM NaCl, 0.5% sodium deoxycholate, 1% TX-100, 5 mM NaF, and one-half tablet of Complete protease inhibitor (Roche Applied Science) in 20 ml of buffer), maintained on ice for 30 min, precleared with protein G beads for 30 min at 4 °C, and then spun at 12,000 rpm for 15 min. Total protein was assessed using the BCA protein assay kit (Pierce). 2 mg of protein lysate was incubated with 2 $\mu$g of anti-Cx32 or mouse IgG (4 h at 4 °C) and then incubated with 100 $\mu$l of protein G–Sepharose (GE Healthcare) (overnight at 4 °C). The Sepharose was washed four times with cold lysis buffer, and the co-IP was analyzed by SDS-PAGE and Western blotting. Anti-EphB1 mAb was used to detect EphB1 co-IP with Cx32.

Protein levels were detected by SDS-PAGE and Western blotting. One exception for detecting tyrosine phosphorylation was that 5 mM $Na_3VO_4$ was added in the blocking buffer and primer antibody buffer to minimize the loss of phosphorylation. Western blotting data were scanned and quantified using ImageJ as described (45).

### GST pulldowns

The GST pulldown assay was modified from that described previously (46). Briefly, purified GST, GST-Cx32NT, or GST-Cx32CT was bound to GSH-Sepharose beads in buffer containing 25 mM Tris-HCl (pH 7.4),150 mM NaCl, 0.1% TX-100, 1 mM DTT, 0.1 mM EDTA, and one-half tablet of Complete protease inhibitor in 20 ml of buffer. 5 mg of either purified TC-PTP(1–314) was incubated with the GST control or either GST fusion protein overnight at 4 °C on a rotating wheel. Beads were washed five times with buffer, and bound proteins were eluted with SDS-PAGE sample buffer and analyzed by Western blotting.

To pull down Cx32-binding partners, 4 mg of MDA-MB-231 cell lysate protein (in cell lysis buffer containing 25 mM Tris-HCl (pH 7.4), 150 mM NaCl, 0.5% TX-100, 0.5% sodium deoxycholate, 2 mM EDTA, PhosSTOP (Roche Applied Science), and Complete protease inhibitor) were incubated with GST-Cx32CT or the GST control for 6 h at 4 °C on a rotating wheel. Beads were washed five times with cell lysis buffer, and bound proteins were eluted with SDS-PAGE sample buffer and analyzed by Western blotting.

### NMR-HSQC experiment

NMR data were acquired using a 600-MHz Varian INOVA NMR spectrometer outfitted with a Bruker cryoprobe at the NMR Facility of the University of Nebraska Medical Center. Cx32CT(217–283) and TC-PTP(1–314) were expressed and purified as described previously (15, 23). Gradient-enhanced two-dimensional $^{15}N$ HSQC experiments were acquired to detect backbone amide bond resonances from the [$^{15}N$]Cx32CT (30 $\mu$M) in the absence and presence of different concentrations of unlabeled TC-PTP(1–314).

## Cx32 (de)phosphorylation

For testing the interaction with CaM, peptides corresponding to Cx32CT(217–266) (not phosphorylated) or Cx32CT(217–266) pTyr$^{243}$ were purchased (LifeTein), and [$^{15}$N]CaM was expressed recombinantly and purified by affinity chromatography using a Phenyl HP column (Amersham Biosciences). Pure CaM was eluted with Tris-EGTA, dialyzed extensively against water, and lyophilized. Gradient-enhanced two-dimensional $^{15}$N HSQC experiments were acquired to detect backbone amide bond resonances from the [$^{15}$N]CaM (30 $\mu$M) in the absence and presence of different concentrations of either unlabeled nonphosphorylated Cx32CT(217–266) or Cx32CT(217–266) pTyr$^{243}$. A similar approach was used to test the impact of pTyr$^{243}$ on the interaction with hDlg. $^{15}$N HSQC experiments were acquired to detect backbone amide bond resonances from [$^{15}$N]Cx32CT WT or Y243E (50 $\mu$M) in the absence and presence of unlabeled SAP97-GUK(701–924) domain. SAP97-GUK(701–924) was purified as described (15). NMR spectra were processed using NMRPipe (47) and analyzed with NMRView (48). Binding affinity from the $^{15}$N HSQC titration experiments was calculated by GraphPad Prism version 5 (GraphPad Software, Inc.).

### *In vitro phosphatase assay*

Cx32 phosphopeptide pTyr$^{243}$ (HRLSPEpYKQNEIN) was used in the Malachite green assay (Millipore) to detect whether they are substrates of TC-PTP *in vitro*. Positive and negative controls were DADEpYL (described previously (49)) and ARKRIpYPP (described previously (50)), respectively. Peptides and enzyme were dissolved and diluted in reaction buffer (60 mM HEPES (pH 7.2), 150 mM NaCl, 1 mM EDTA, 0.17 mM DTT, 0.83% glycerol, 0.017% BSA, and 0.002% Brij-35) and temperature-equilibrated for 15 min at RT. A 500 $\mu$M concentration of each peptide was added into a 96-well plate, and then TC-PTP(1–314) was added to each peptide at different time points. The final concentration of TC-PTP(1–314) was 0.6 nM. All reactions were terminated by adding 100 $\mu$l of Malachite green solution and incubated for 15 min at RT to allow color development. Absorbance at 650 nm was read using a SpectraMax 190 spectrometer (Molecular Devices).

The Malachite green assay was also used to measure the kinetic parameters of dephosphorylation (49). The reaction was performed in 96-well plates with a final volume of 25 $\mu$l. A standard curve of $KH_2PO_4$, used for calculating the release of $P_i$, was determined on the same plate as the reaction samples. Different concentrations of peptides, [substrate], were combined with 1.2 nmol of TC-PTP(1–314). Time points of the reaction were sampled from 0 to 15 min to calculate the initial velocity ($v$) *versus* [substrate]. A Lineweaver–Burk double-reciprocal plot (rearranged from the Michaelis–Menten equation) was created based on 1/$v$ and 1/[substrate]. The kinetic parameters were determined by the linear equation from the Lineweaver–Burk double-reciprocal plot. All of the reactions were conducted at pH 7.5, 25 °C. The reported results were calculated from three independent experiments.

### *Scrape-loading assay*

Cells were scrape-loaded as described (15). Briefly, both HeLa cells expressing Cx32 WT or the Y243E mutant and Caco2 cells were seeded on coverslips 24 h before performing the assay. Cell culture medium from 100% confluent cells was removed and replaced with 1 ml of PBS containing 0.25% Lucifer yellow and Texas Red–conjugated fluorescent dextran (10 kDa, 1.5 mg/ml; fixable). Cells were scrape-loaded with a sterile scalpel by two longitudinal scratches and then incubated at RT for 1 min for HeLa cells and 4 min for Caco2. Cells were washed quickly three times with warm PBS (containing $MgCl_2$ and $CaCl_2$) or cell culture medium followed by incubation at 37 °C for 5 min. After incubation, cells were washed two times with warm PBS and fixed with 3.7% buffered paraformaldehyde for 15 min. 0.1 M glycine was used to quench autofluorescence for 15 min. Coverslips were mounted on glass slides in a droplet of SlowFade (Invitrogen). The result was confirmed by repeating the experiment three times and for each trial, capturing four side-by-side images. The method to quantify dye transfer was described previously (15). Briefly, cells with Lucifer yellow were counted, whereas the cells with dextran, which indicated the initially loaded cells, were excluded.

### *Statistical analysis*

All data were analyzed by GraphPad Prism version 5.0 and presented as the mean ± S.D. Either Student's $t$ test or one-way ANOVA with Neuman–Keuls *post hoc* analysis was used to compare differences between all groups where appropriate. $p < 0.05$ was considered to be statistically significant.

*Author contributions*—A. J. T., H. L., G. S., L. Z., and K. L. S. data curation; A. J. T., H. L., G. S., and L. Z. formal analysis; A. J. T., G. S., and P. L. S. writing-review and editing; P. L. S. conceptualization; P. L. S. resources; P. L. S. supervision; P. L. S. funding acquisition; P. L. S. writing-original draft; P. L. S. project administration.

*Acknowledgments—We thank Janice A. Taylor and James R. Talaska (Advanced Microscopy Core Facility, University of Nebraska Medical Center) for providing assistance with confocal microscopy.*

### References

1. Fowler, S. L., McLean, A. C., and Bennett, S. A. (2009) Tissue-specific cross-reactivity of connexin32 antibodies: problems and solutions unique to the central nervous system. *Cell Commun. Adhes.* **16,** 117–130 Medline
2. Temme, A., Buchmann, A., Gabriel, H. D., Nelles, E., Schwarz, M., and Willecke, K. (1997) High incidence of spontaneous and chemically induced liver tumors in mice deficient for connexin32. *Curr. Biol.* **7,** 713–716 CrossRef Medline
3. King, T. J., and Lampe, P. D. (2004) Mice deficient for the gap junction protein Connexin32 exhibit increased radiation-induced tumorigenesis associated with elevated mitogen-activated protein kinase (p44/Erk1, p42/Erk2) activation. *Carcinogenesis* **25,** 669–680 CrossRef Medline
4. Temme, A., Stümpel, F., Söhl, G., Rieber, E. P., Jungermann, K., Willecke, K., and Ott, T. (2001) Dilated bile canaliculi and attenuated decrease of nerve-dependent bile secretion in connexin32-deficient mouse liver. *Pflugers Arch.* **442,** 961–966 CrossRef Medline
5. Chanson, M., Fanjul, M., Bosco, D., Nelles, E., Suter, S., Willecke, K., and Meda, P. (1998) Enhanced secretion of amylase from exocrine pancreas of connexin32-deficient mice. *J. Cell Biol.* **141,** 1267–1275 CrossRef Medline
6. Scherer, S. S., Xu, Y. T., Nelles, E., Fischbeck, K., Willecke, K., and Bone, L. J. (1998) Connexin32-null mice develop demyelinating peripheral neuropathy. *Glia* **24,** 8–20 CrossRef Medline
7. King, T. J., and Lampe, P. D. (2004) The gap junction protein connexin32 is a mouse lung tumor suppressor. *Cancer Res.* **64,** 7191–7196 CrossRef Medline

8. Scherer, S. S., and Kleopa, K. A. (2012) X-linked Charcot-Marie-Tooth disease. *J. Peripher. Nerv. Syst.* **17,** 9–13 CrossRef Medline
9. Kleopa, K. A., Abrams, C. K., and Scherer, S. S. (2012) How do mutations in GJB1 cause X-linked Charcot-Marie-Tooth disease? *Brain Res.* **1487,** 198–205 CrossRef Medline
10. Solan, J. L., and Lampe, P. D. (2014) Specific Cx43 phosphorylation events regulate gap junction turnover *in vivo*. *FEBS Lett.* **588,** 1423–1429 CrossRef Medline
11. Díez, J. A., Elvira, M., and Villalobo, A. (1995) Phosphorylation of connexin-32 by the epidermal growth factor receptor tyrosine kinase. *Ann. N.Y. Acad. Sci.* **766,** 477–480 CrossRef Medline
12. Sáez, J. C., Nairn, A. C., Czernik, A. J., Spray, D. C., Hertzberg, E. L., Greengard, P., and Bennett, M. V. (1990) Phosphorylation of connexin 32, a hepatocyte gap-junction protein, by cAMP-dependent protein kinase, protein kinase C and $Ca^{2+}$/calmodulin-dependent protein kinase II. *Eur. J. Biochem.* **192,** 263–273 CrossRef Medline
13. Takeda, A., Hashimoto, E., Yamamura, H., and Shimazu, T. (1987) Phosphorylation of liver gap junction protein by protein kinase C. *FEBS Lett.* **210,** 169–172 CrossRef Medline
14. Seo, M. S., Park, J. S., Yang, S. R., Park, K. S., Hong, I. S., Jo, E. H., Kang, K. S., and Lee, Y. S. (2006) Expression of MAP kinases and connexins in the differentiation of rat mammary epithelial cells. *J. Vet. Med. Sci.* **68,** 567–571 CrossRef Medline
15. Stauch, K., Kieken, F., and Sorgen, P. (2012) Characterization of the structure and intermolecular interactions between the connexin 32 carboxyl-terminal domain and the protein partners synapse-associated protein 97 and calmodulin. *J. Biol. Chem.* **287,** 27771–27788 CrossRef Medline
16. Locke, D., Koreen, I. V., and Harris, A. L. (2006) Isoelectric points and post-translational modifications of connexin26 and connexin32. *FASEB J.* **20,** 1221–1223 CrossRef Medline
17. Poliakov, A., Cotrina, M., and Wilkinson, D. G. (2004) Diverse roles of eph receptors and ephrins in the regulation of cell migration and tissue assembly. *Dev. Cell* **7,** 465–480 CrossRef Medline
18. Pasquale, E. B. (2008) Eph-ephrin bidirectional signaling in physiology and disease. *Cell* **133,** 38–52 CrossRef Medline
19. Davy, A., Bush, J. O., and Soriano, P. (2006) Inhibition of gap junction communication at ectopic Eph/ephrin boundaries underlies craniofrontonasal syndrome. *PLoS Biol.* **4,** e315 CrossRef Medline
20. Mellitzer, G., Xu, Q., and Wilkinson, D. G. (1999) Eph receptors and ephrins restrict cell intermingling and communication. *Nature* **400,** 77–81 CrossRef Medline
21. Ishii, M., Mueller, I., Nakajima, T., Pasquale, E. B., and Ogawa, K. (2011) EphB signaling inhibits gap junctional intercellular communication and synchronized contraction in cultured cardiomyocytes. *Basic Res. Cardiol.* **106,** 1057–1068 CrossRef Medline
22. Liu, H., Huang, R. Y., Chen, J., Gross, M. L., and Pakrasi, H. B. (2011) Psb27, a transiently associated protein, binds to the chlorophyll binding protein CP43 in photosystem II assembly intermediates. *Proc. Natl. Acad. Sci. U.S.A.* **108,** 18536–18541 CrossRef Medline
23. Li, H., Spagnol, G., Naslavsky, N., Caplan, S., and Sorgen, P. L. (2014) TC-PTP directly interacts with connexin43 to regulate gap junction intercellular communication. *J. Cell Sci.* **127,** 3269–3279 CrossRef Medline
24. Remo, B. F., Qu, J., Volpicelli, F. M., Giovannone, S., Shin, D., Lader, J., Liu, F. Y., Zhang, J., Lent, D. S., Morley, G. E., and Fishman, G. I. (2011) Phosphatase-resistant gap junctions inhibit pathological remodeling and prevent arrhythmias. *Circ. Res.* **108,** 1459–1466 CrossRef Medline
25. Solan, J. L., Marquez-Rosado, L., Sorgen, P. L., Thornton, P. J., Gafken, P. R., and Lampe, P. D. (2007) Phosphorylation at S365 is a gatekeeper event that changes the structure of Cx43 and prevents down-regulation by PKC. *J. Cell Biol.* **179,** 1301–1309 CrossRef Medline
26. Spagnol, G., Kieken, F., Kopanic, J. L., Li, H., Zach, S., Stauch, K. L., Grosely, R., and Sorgen, P. L. (2016) Structural studies of the Nedd4 WW domains and their selectivity for the Cx43 carboxyl-terminus. *J. Biol. Chem.* **291,** 7637–7650 CrossRef Medline
27. Ambrosi, C., Ren, C., Spagnol, G., Cavin, G., Cone, A., Grintsevich, E. E., Sosinsky, G. E., and Sorgen, P. L. (2016) Connexin43 forms supramolecular complexes through non-overlapping binding sites for drebrin, tubulin, and ZO-1. *PLoS One* **11,** e0157073 CrossRef Medline
28. Peracchia, C., Sotkis, A., Wang, X. G., Peracchia, L. L., and Persechini, A. (2000) Calmodulin directly gates gap junction channels. *J. Biol. Chem.* **275,** 26220–26224 CrossRef Medline
29. Peracchia, C., Wang, X. G., and Peracchia, L. L. (2000) Slow gating of gap junction channels and calmodulin. *J. Membr. Biol.* **178,** 55–70 CrossRef Medline
30. Díez, J. A., Elvira, M., and Villalobo, A. (1998) The epidermal growth factor receptor tyrosine kinase phosphorylates connexin32. *Mol. Cell Biochem.* **187,** 201–210 CrossRef Medline
31. Konstantinova, I., Nikolova, G., Ohara-Imaizumi, M., Meda, P., Kucera, T., Zarbalis, K., Wurst, W., Nagamatsu, S., and Lammert, E. (2007) EphA-Ephrin-A-mediated $\beta$ cell communication regulates insulin secretion from pancreatic islets. *Cell* **129,** 359–370 CrossRef Medline
32. Atkinson, M. M., Menko, A. S., Johnson, R. G., Sheppard, J. R., and Sheridan, J. D. (1981) Rapid and reversible reduction of junctional permeability in cells infected with a temperature-sensitive mutant of avian sarcoma virus. *J. Cell Biol.* **91,** 573–578 CrossRef Medline
33. Atkinson, M. M., and Sheridan, J. D. (1988) Altered junctional permeability between cells transformed by v-ras, v-mos, or v-src. *Am. J. Physiol.* **255,** C674–C683 CrossRef Medline
34. Lau, A. F., Kurata, W. E., Kanemitsu, M. Y., Loo, L. W., Warn-Cramer, B. J., Eckhart, W., and Lampe, P. D. (1996) Regulation of connexin43 function by activated tyrosine protein kinases. *J. Bioenerg. Biomembr.* **28,** 359–368 CrossRef Medline
35. Solan, J. L., and Lampe, P. D. (2008) Connexin 43 in LA-25 cells with active v-src is phosphorylated on Y247, Y265, S262, S279/282, and S368 via multiple signaling pathways. *Cell Commun. Adhes.* **15,** 75–84 CrossRef Medline
36. Li, H., Spagnol, G., Zheng, L., Stauch, K. L., and Sorgen, P. L. (2016) Regulation of Connexin43 function and expression by tyrosine kinase 2. *J. Biol. Chem.* **291,** 15867–15880 CrossRef Medline
37. Burt, J. M., and Spray, D. C. (1988) Inotropic agents modulate gap junctional conductance between cardiac myocytes. *Am. J. Physiol.* **254,** H1206–H1210 Medline
38. van Veen, T. A., van Rijen, H. V., and Jongsma, H. J. (2000) Electrical conductance of mouse connexin45 gap junction channels is modulated by phosphorylation. *Cardiovasc. Res.* **46,** 496–510 CrossRef Medline
39. Jacobsen, N. L., Pontifex, T. K., Li, H., Solan, J. L., Lampe, P. D., Sorgen, P. L., and Burt, J. M. (2017) Regulation of Cx37 channel and growth suppressive properties by phosphorylation. *J. Cell Sci.* **130,** 3308–3321 CrossRef Medline
40. Thul, P. J., and Lindskog, C. (2018) The human protein atlas: a spatial map of the human proteome. *Protein Sci.* **27,** 233–244 CrossRef Medline
41. Lisabeth, E. M., Falivelli, G., and Pasquale, E. B. (2013) Eph receptor signaling and ephrins. *Cold Spring Harb. Perspect. Biol.* **5,** a009159 CrossRef Medline
42. Funk, S. D., and Orr, A. W. (2013) Ephs and ephrins resurface in inflammation, immunity, and atherosclerosis. *Pharmacol. Res.* **67,** 42–52 CrossRef Medline
43. Coulthard, M. G., Morgan, M., Woodruff, T. M., Arumugam, T. V., Taylor, S. M., Carpenter, T. C., Lackmann, M., and Boyd, A. W. (2012) Eph/Ephrin signaling in injury and inflammation. *Am. J. Pathol.* **181,** 1493–1503 CrossRef Medline
44. Solan, J. L., and Lampe, P. D. (2016) Kinase programs spatiotemporally regulate gap junction assembly and disassembly: effects on wound repair. *Semin. Cell Dev. Biol.* **50,** 40–48 CrossRef Medline
45. Trease, A. J., Capuccino, J. M. V., Contreras, J., Harris, A. L., and Sorgen, P. L. (2017) Intramolecular signaling in a cardiac connexin: role of cytoplasmic domain dimerization. *J. Mol. Cell Cardiol.* **111,** 69–80 CrossRef Medline
46. Leykauf, K., Salek, M., Bomke, J., Frech, M., Lehmann, W. D., Dürst, M., and Alonso, A. (2006) Ubiquitin protein ligase Nedd4 binds to connexin43 by a phosphorylation-modulated process. *J. Cell Sci.* **119,** 3634–3642 CrossRef Medline
47. Delaglio, F., Grzesiek, S., Vuister, G. W., Zhu, G., Pfeifer, J., and Bax, A. (1995) NMRPipe: a multidimensional spectral processing system based on UNIX pipes. *J. Biomol. NMR* **6,** 277–293 Medline

48. Johnson, B. A., and Blevins, R. A. (1994) NMR View: a computer program for the visualization and analysis of NMR data. *J. Biomol. NMR* **4,** 603–614 CrossRef Medline
49. Peters, N. S., and Wit, A. L. (2000) Gap junction remodeling in infarction: does it play a role in arrhythmogenesis? *J. Cardiovasc. Electrophysiol.* **11,** 488–490 CrossRef Medline
50. Ren, L., Chen, X., Luechapanichkul, R., Selner, N. G., Meyer, T. M., Wavreille, A. S., Chan, R., Iorio, C., Zhou, X., Neel, B. G., and Pei, D. (2011) Substrate specificity of protein tyrosine phosphatases 1B, RPTPα, SHP-1, and SHP-2. *Biochemistry* **50,** 2339–2356 CrossRef Medline
51. Uhlen, M., Fagerberg, L., Hallstrom, B. M., Lindskog, C., Oksvold, P., Mardinoglu, A., Sivertsson, A., Kampf, C., Sjostedt, E., Asplund, A., Olsson, I., Edlund, K., Lundberg, E., Navani, S., Szigyarto, C. A., *et al.* (2015) Proteomics: tissue-based map of the human proteome. *Science* **347,** 1260419 CrossRef Medline
52. Peters, G. H., Iversen, L. F., Branner, S., Andersen, H. S., Mortensen, S. B., Olsen, O. H., Moller, K. B., and Moller, N. P. (2000) Residue 259 is a key determinant of substrate specificity of protein-tyrosine phosphatases 1B and α. *J. Biol. Chem.* **275,** 18201–18209 CrossRef Medline